Bulk Nuclear Polarization Enhanced at Room-Temperature by Optical Pumping

Ran Fischer,[1] Christian O. Bretschneider,[2] Paz London,[1] Dmitry Budker,[3,4] David Gershoni,[1] and Lucio Frydman[2,*]

[1]*Department of Physics, Technion, Israel Institute of Technology, Haifa, 32000, Israel*
[2]*Department of Chemical Physics, Weizmann Institute of Science, Rehovot, 76100, Israel*
[3]*Department of Physics, University of California, Berkeley, CA, 94720-7300, USA*
[4]*Nuclear Science Division, Lawrence Berkeley National Laboratory, CA, 94720, USA*

Bulk ^{13}C polarization can be strongly enhanced in diamond at room-temperature based on the optical pumping of nitrogen-vacancy color centers. This effect was confirmed by irradiating suitably aligned single-crystals placed at a ∼50 mT field, rapidly shuttling the sample into a custom-built NMR setup, and subsequent ^{13}C detection. A nuclear polarization of ∼0.4% - equivalent to the ^{13}C polarization achievable by thermal means at fields of ∼2000 T - was measured, and its bulk nature determined based on chemical shift and relaxation measurements. The enhanced polarization strongly depends on the magnitude of the magnetic field, including sign alterations, due to the anisotropic nature of the NV- nuclei coupling. Owing to its simplicity, this ^{13}C room-temperature polarizing strategy provides a promising new addition to existing nuclear hyperpolarization techniques.

PACS numbers: 61.72.jn, 76.60.-k, 78.47.-p, 81.05.ug

Introduction.— Nuclear Magnetic Resonance (NMR) is commonly used to extract molecular-level information in a wide variety of physical, chemical and biological scenarios. One of NMR's most distinctive characteristics is the low energies it involves. This makes the method remarkably non-invasive but leads to intrinsically low signal-to-noise ratios (SNR's), factoring in both small thermal spin polarizations and relatively low frequencies. Over the last decades several strategies have been proposed to bypass these limitations; - particularly by generating large, non-thermal spin-polarized states. Most prominent among these techniques is Dynamic Nuclear Polarization (DNP) [1–6], where radicals are irradiated in a high-field cryogenic environment, driving their unpaired electron spins away from equilibrium and thereby leading to highly-polarized nuclei on co-mixed, nearby target molecules. This and other forms of hyperpolarization can increase the NMR/MRI signals by several orders of magnitude, promising to significantly expand these spectroscopies' scope of applications in chemistry and biomedicine [7]. In the past, free radicals arising in imperfect diamond crystals have also been the target of cryogenic DNP NMR investigations [8]. Those studies have been recently extended to exploit the electronic spin states of negatively-charged Nitrogen-Vacancy (NV) centers in diamond. These color centers have been proposed for a variety of applications including spintronics [9–13] and in ultrasensitive magnetometers [14–17]. A particularly appealing aspect of NV-doped diamonds is the simplicity with which they can deliver highly polarized electronic populations by optical pumping at room temperature: several studies have demonstrated that the ensuing electronic spin order can be transferred via hyperfine interactions to nearby nuclei [18–22]. In this study we extend such observations by exploring characteristics of the polarization transfer between the optically pumped electronic spin states in NV centers, to the bulk ^{13}C nuclei of the diamond. To this end, the m_s = 0 excited state of the NV center was optically pumped by laser irradiation, and the electronic spin polarization was transferred to ^{13}C by suitably orienting the diamond crystal at a field of around 50 mT. This transfer of order between the electronic and nuclear spins is known to polarize ^{13}C spins located in close vicinity to the NV centers [18, 23–25]. Here we show that the polarization is transferred to the bulk nuclei as well. To this effect we use an experimental setup which rapidly transfers optically pumped NV-doped diamonds to a 4.7 T field, where the ^{13}C spins are excited using an on-resonant radiofrequency (RF) pulse. The nuclear spins are then detected by conventional NMR induction at 50.55 MHz. The detected signal exceeds by two-three orders of magnitude the signal observed in the same setup after the sample was subject to full thermal relaxation in a 4.7 T field. We established that this signal arose from bulk, as opposed to NV-localized, ^{13}C polarization, based on the identical spin-lattice relaxation and chemical shift characteristics of pumped vs. non-pumped ^{13}C magnetization at a variety of high fields. In addition, we observed that the nuclear polarization has a complex dependence on the magnetic field during the optical pumping. This dependence, including its sign alternations, could be explained by the anisotropic nature of the electron-nuclear hyperfine interaction.

^{13}C Polarization Enhancement in Optically Pumped Diamonds. — The negatively charged NV color center in diamond is composed of a substitutional nitrogen atom associated with an adjacent lattice vacancy. This center is characterized by an electronic spin-triplet in the ground ($^3A_2$) and excited (^{3}E) state. At room temperature these S = 1 states exhibit zero-field splittings between the m_S = 0 and the m_S = ±1 spin sublevels of 2.87 GHz and 1.42 GHz, respectively (Fig. 1a). Optical transitions are primarily spin conserving [27, 28]. However, the presence of a non-radiative, spin-selective relaxation mechanism involving an intersystem crossing with singlet levels, can alter the

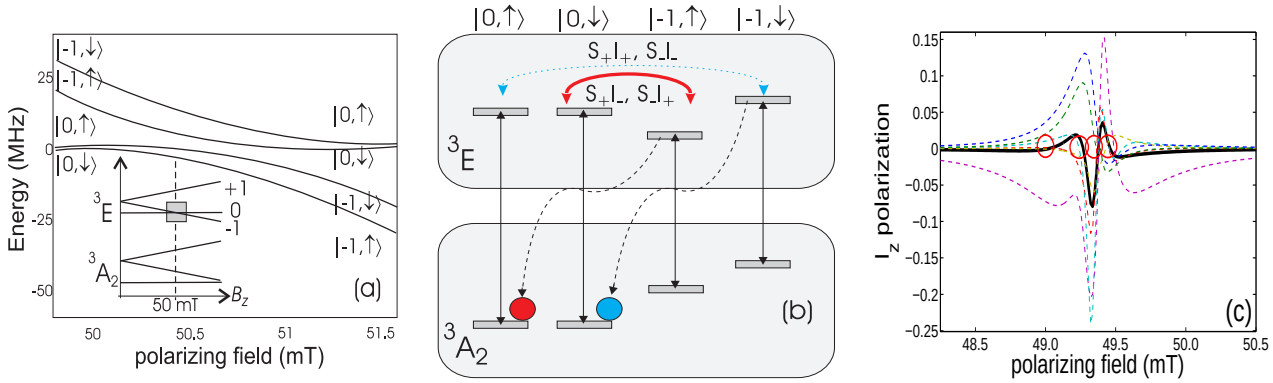

Figure 1: (Color online) (a) Schematic energy diagram of the electronic ground ($^3A_2$) and excited (^3E) triplet states of an NV center at room-temperature as a function of an axial magnetic field B_z. The magnified sketch shows the region at approximately 50 mT in which level anti-crossings occur in between the excited state sub-levels. The electronic sub-states m_s = 0 and m_s = 1 exhibit additional splittings due to hyperfine and nuclear Zeeman interactions. (b) Simplified schematic description of the polarization transfer processes between the electronic and nuclear sub-states under optical pumping in the presence of a hyperfine interaction. Black solid and dashed arrows represent optical and spin-selective relaxation transitions and red (cyan) arrows illustrate the mixing of the $|\text{-}1,\uparrow\rangle$ and $|0,\uparrow\rangle$ ($|\text{-}1,\downarrow\rangle$ and $|0,\downarrow\rangle$) energy levels, resulting in a positive (negative) nuclear polarization. (c) Expected nuclear polarizations of proximal ^{13}C spins as a function of an axial magnetic field as determined by density matrix model simulations. The bold line describes the mean polarization resulting by averaging over six individual orientations of the hyperfine tensor (dashed lines) [26]. Further details on this calculation can be found in the Supplementary Information. Notice the multiple zero crossings (red circles) of the nuclear polarization due to averaging over sub-ensembles with different hyperfine tensors.

electronic spin populations. Under suitable optical irradiation the ensuing pumping can be very effective, leading even at room-temperature, to a nearly full population of the m_s = 0 electronic states. This electronic spin order can be transferred to nearby ^{13}C in the diamond lattice (Fig. 1b). To envision the nature of this transfer, we neglect for simplicity the ^{14}N-related spin interactions, and consider a single NV-^{13}C spin Hamiltonian

$$\hat{H} = D_{ES}\hat{S}_z^2 + (\gamma_{NV}\hat{S}_z + \gamma_{^{13}C}\hat{I}_z)\vec{B} + \hat{S}\cdot A_{IS}\cdot\hat{I}. \quad (1)$$

Here $\hat{I}$ and $\hat{S}$ are the nuclear and electron spin operators, D_{ES} is the excited-state zero-field splitting, γ_{NV} = 2.8·10^4 MHz/T and $\gamma_{^{13}C}$ = 10 MHz/T are the corresponding gyromagnetic ratios, and A_{IS} is the hyperfine tensor. It is also assumed that a positive, axial magnetic field $\vec{B}$ = B_z has been aligned with the NV axis (as was experimentally the case), leaving the electronic spin an eigenstate of $\hat{S}_z$. The zero-field and electronic Zeeman splitting dominate Eq. (1), thereby generally quenching electronic $\leftrightarrow$ nuclear spin exchange. Still, as illustrated in Figs. 1(a), the energy levels change with B_z. At a field of 50 mT the contributions of these two dominant electronic terms balance out for the electronic $\{|0\rangle, |\text{-}1\rangle\}$ subspace, resulting in an anti-crossing dominated by the hyperfine interaction with nearby nuclear spins. This in turn, can lead to a transfer between pumped electronic and the nuclear spin populations $\{|\uparrow\rangle,|\downarrow\rangle\}$. Indeed, when $||D_{ES} - \gamma_{NV}B_z| \pm \gamma_{^{13}C}B_z| < |A_{IS}|$, the electronic spin is no longer an eigenstate of $\hat{H}$. The system can still be described in a joint manifold of the nuclear and electronic spins, but the eigenstates of $\hat{H}$ under these conditions will be a mixture of the $|0,\uparrow\rangle$, $|0,\downarrow\rangle$, $|\text{-}1,\uparrow\rangle$ and $|\text{-}1,\downarrow\rangle$ states. If A_{IS} is a so-called isotropic hyperfine interaction possessing solely $\hat{S}_+\hat{I}_-$, $\hat{S}_-\hat{I}_+$ "zero-quantum" terms, only the $|\text{-}1,\uparrow\rangle$ and $|0,\downarrow\rangle$ states will be mixed by the level anti-crossing, leading to an enrichment of the nuclear $|\uparrow\rangle$ state upon optical pumping (Fig. 1b). By contrast, ^{13}C's proximal to NV centers exhibit an anisotropic hyperfine interaction [29], resulting in an additional mixing of states involving single- and double-quantum operators $\hat{S}_z\hat{I}_\pm$, $\hat{S}_\pm\hat{I}_z$, $\hat{S}_+\hat{I}_+$ and $\hat{S}_-\hat{I}_-$. Under optical pumping, zero- and double quantum terms can drive the nuclei into either polarized or anti-polarized states (Fig. 1b), whose dominance will be given by the magnitude of $\vec{B}$ and by the characteristics of A_{IS}. This is illustrated by the simulations in Figs. 1(c), which show multiple sign alterations in the nuclear spin polarization as a function of the polarizing field. Equation (1) and the processes depicted in Fig. 1 approximate the polarization of the ^{13}C nuclear spins in the immediate proximity of the NV centers. For a majority of ^{13}C in a macroscopic ensemble, however, A_{IS} are too small to enable a significant inter-spin polarization transfer due to the short lifetime of the excited state ($\sim$10 ns). This notwithstanding, it is conceivable that nuclear spin-diffusion events driven by $(\hat{I}_{1+}\hat{I}_{2-} + \hat{I}_{1-}\hat{I}_{2+})$-like terms originating from the nuclear dipole-dipole interaction, can successfully transfer the nuclear polarization from the neighborhood of the NV-centers to the bulk ^{13}C nuclei. Such processes would have to defeat nuclear T_1 effects in order to be efficient. To investigate the existence of this polarization transfer mechanism, which

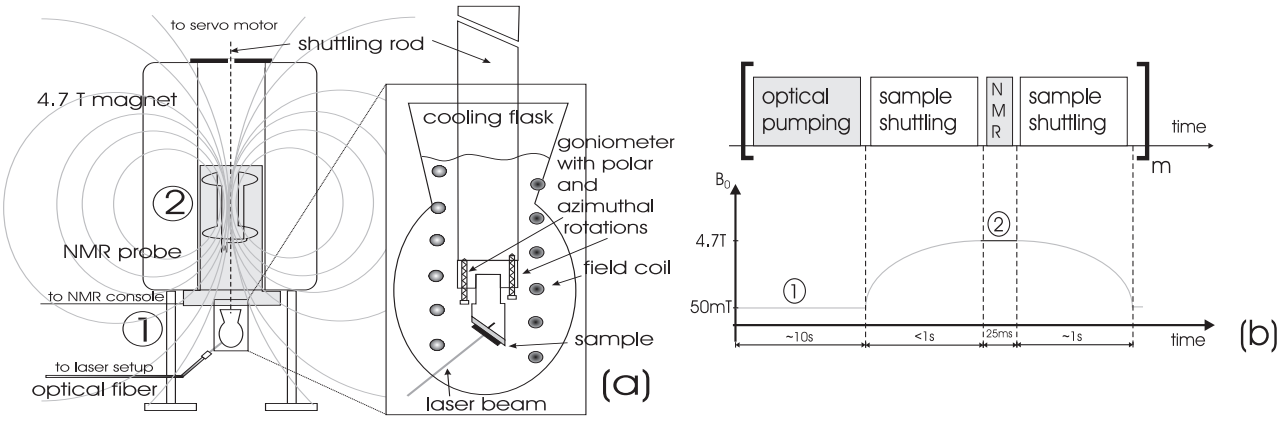

Figure 2: (a-b) Schematic description of the experimental setup and a summary of the events during the experiments. The acquisition cycle begins with a laser pumping of the electronic spins, followed by a polarization transfer to nuclear spins facilitated in a suitable 50 mT B_z field. This is followed by shuttling the sample from the polarizing field ① to the "sweet spot" of a high-field magnet ②, where the ^{13}C spins are subject to a pulsed spin-echo detection. The sample was then returned to the polarizing field for a repeated pumping and further signal averaging. The samples used (D01 and D02) are synthetic diamond single-crystals (3 mm*3 mm*0.5 mm), with a natural abundance of ^{13}C and an initial nitrogen concentration of less than 200 ppm. NV centers were generated through electron irradiation (10 MeV electrons with a dose of 10^{18} cm^{-2}), followed by subsequent annealing of the sample at 1000 °C for 2 hours. Fluorescence measurements suggested a three times higher concentration of NV centers in D02 compared to D01. The pumping laser was connected to the optical setup via a 600 μm multimode fiber irradiating the diamond sample with a 532 nm laser beam with an adjustable power of up to 10 W, distributed equally over the whole sample. The setup was used for NMR and ODMR measurements (for more details see the Supplementary Information). The diamond was mounted on a holder and carefully aligned to make the polarizing field purely axial relative to one crystallographic orientation of the NV centers. The field was fine-tuned via an ancillary coil. The sample was immersed in a water-filled flask maintained at a temperature below 50°C while illuminated with laser light, and connected by a shuttling rod to a servo motor enabling its transfer (in <1s) into and out of the high-field NMR setup. The data were acquired using a custom-built NMR probe enabling free shuttling through a 12 mm Helmholtz coil configuration tuned to 50.55 MHz, both from the top and bottom of the magnet.

could enable bulk nuclear polarization by optical means, we assembled the setup illustrated in Fig. 2(a). The associated experiment began with careful positioning and alignment of an NV center-endowed diamond single crystal, in a $B_z \sim 50$ mT field fulfilling the excited-state anti-crossing conditions described above (for more details see the Supplementary Information). Following laser irradiation of the color centers and pumping of the electronic populations to the m_s = 0 state - and the build-up of nuclear spin polarization as per Fig. 1(c) - the experiment continued with a mechanical shuttling of the sample within sub-second timescales from the polarizing field to a detection field (4.7 T), via a servo motor controlled by an NMR console. This motion positioned the diamond crystal within a ^{13}C-tuned Helmholtz-coil circuit; as soon as the sample reached this coil an NMR spin-echo sequence was applied to probe the level of bulk ^{13}C magnetization. Such pump-shuttle-pulse process could be repeated numerous times for the sake of signal averaging.

Results and Discussion.— It follows from bulk NMR measurements of the diamond crystal dubbed D01 (D02) (Fig. 3a), that approximately 0.1% (0.4%) of the electronic spin polarization can be transferred to the bulk of the ^{13}C spin ensemble, which corresponds to an enhancement factor of 100 (400). Taking into account the different polarizing/observation field strengths, the overall enhancement at 50 mT is > 10000. This hyperpolarized signal and signal arising from thermal high-field Boltzmann ^{13}C magnetizations show the same characteristics; their chemical shift (Fig. 3a) as well as their spin-lattice relaxation times, are identical within experimental errors (Fig. 3b, 3c). Thus, we conclude that the observed hyperpolarized signal originates from the ^{13}C bulk nuclei rather from a subset of nuclei in the immediate vicinity of the color centers. By contrast, if the ^{13}C signal were to arise from the immediate surroundings of the NV center, a much shorter relaxation time would be expected driven by paramagnetic relaxation mechanisms [30, 31]. Interestingly, the spin-lattice relaxation times at B_0 = 4.7 T are two orders of magnitude longer than these at the 50 mT optical pumping field ($T_1^{LowField}$ = 2.5 s, $T_1^{HighField}$ = 125 s). As illustrated in Fig. 3(d), the short nuclear relaxation time at 50 mT ultimately limits the polarization transfer. As evidenced in Fig. 3(e) the overall nuclear polarization also dependends on the laser power.

From a spin-physics standpoint, it is interesting to note that the relative sign of the ^{13}C bulk magnetization can be controlled by scanning the polarization field. This stems from the hyperfine interaction which controls the electronic-nuclear spin transfer, as reflected by the simulations in Fig. 1(c). This effect is demonstrated experimentally in Fig. 3(f), which shows how by applying a

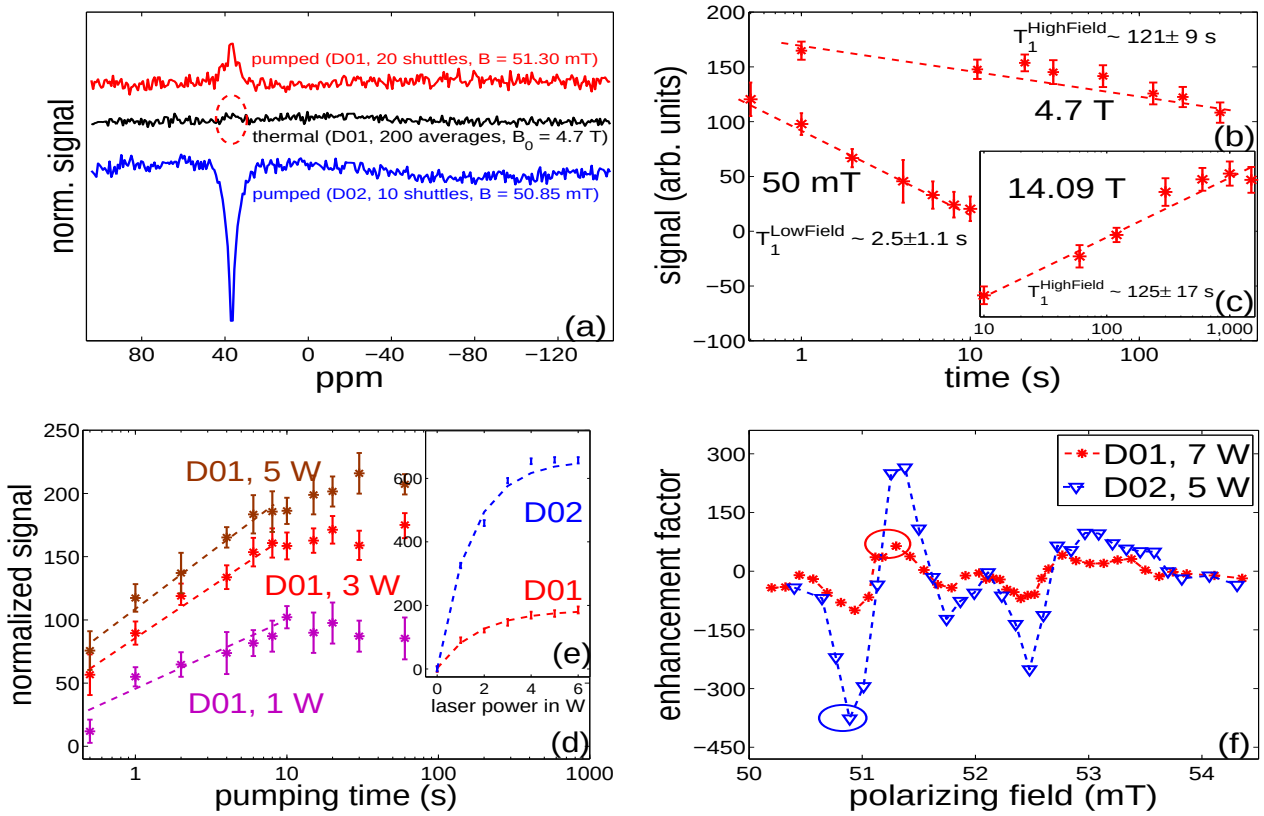

Figure 3: (Color online) Measured experimental data of the diamond samples D01 (red lines, asterisks) and D02 (blue lines, triangles). The dashed lines are guides for the eye. (a) Bulk ^{13}C signal (red and blue line) obtained after 10s of optical pumping and ^{13}C signal acquired with signal averaging at 4.7 T (black line). The SNR after optical pumping is enhanced by up to a factor of 100 (D01) and 400 (D02) compared to the SNR from fully-relaxed, high-field, thermal equilibrium signal. Taking into account the different field strengths the overall enhancement at 50 mT is >10,000. (b) Spin-lattice relaxation characteristics of the optically pumped signal of the sample D01. The longitudinal relaxation of the bulk ^{13}C polarization was measured at the two turning points of the shuttling process -illustrated as ① and ② in Fig. 2(a), 2(b): the polarizing field, and the observation field (see the Supplementary Information for similar data from sample D02). (c) Saturation-recovery of bulk ^{13}C obtained under conventional thermal polarizing conditions on a higher-field solid-state spectrometer (B_0 = 14.09 T). (d-e) Build-up characteristics of the optically pumped bulk ^{13}C polarization as a function of the irradiation time for various laser-beam power and 10 s of pumping. The build-up of the former curve is limited by $T_1^{LowField}$ and evolves into a steady-state. (f) The enhancement of the bulk ^{13}C SNR as a function of the polarizing field. Identical sign alterations are observed for both diamond samples (spectra shown in panel (a) correspond to the encircled points: red circle B_z = 51.30 mT, blue circle B_z = 50.85 mT).

current through the ancillary field coil located around the sample, the bulk ^{13}C signal response can be modulated. The pattern observed in Fig. 3(f) resembles the predictions of Eq. (1), but exhibits several additional minor zero-crossings. These sign alterations in the nuclear polarization were identical for both diamond crystals D01 and D02 (Fig. 3f). This implies that the observed bulk nuclear polarization sign alterations can be interpreted as manifestations of a universal complex behavior that the multiple ^{13}C sub-species coupled by the anisotropic hyperfine interaction with an NV center, will undergo at each resonance instance [24]. Indeed, the possible positions of ^{13}C nuclei in the diamond structure with respect to each NV center, result in an array of individual hyperfine interactions. Therefore, different magnetic field conditions result in efficient electronic-nuclear polarization transfers. A simple density-matrix simulation including multiple proximal spins based on the Hamiltonian of Eq. (1) (Fig. 1c), already provides hints of this complexity. This occurrence of multiple sign alterations in the nuclear spin polarization contrasts with the magnetic field dependence of ^{15}N nuclear spin polarizations [18]: ^{15}N exhibits a nearly isotropic hyperfine interaction, and thus only a positive nuclear spin polarization is observed.

Conclusions.— This study shows that in a single-crystal room temperature diamond, a significant ^{13}C nuclear polarization can be established within seconds, by optical pumping of NV centers at a suitable magnetic field. From this observation, many additional interesting paths emerge to exploit possible synergies between this method of spin

cooling and magnetic resonance experiments. Foremost among these are alternative routes to enhance even further the bulk ^{13}C polarization; either by manipulating the concentration of NV centers, by ^{13}C enrichment, or by choosing different irradiation, field or temperature conditions during the pumping. In addition, strategies can be envisioned for transferring the ^{13}C polarization from the diamond to other molecules, or for using the diamond as a reporter of NMR properties while remaining at low magnetic fields. Interesting opportunities for studies of basic characteristics of spin-spin driven transfers within the diamond as well as to chemical and biological interesting molecules are opened. These and other alternatives to enable a better understanding and a widespread use of this pre-polarizing technique, are being investigated.

The authors are grateful to S. Vega for the fruitful discussions. This research was supported by DIP PRoject 710907 (Ministry of Education and Research, Germany), the EU (through ERC Advanced Grant # 246754), a Helen and Kimmel Award for Innovative Investigation, the IMOD, the National Science Foundation (D.B.) and the generosity of the Perlman Family Foundation.

* E-mail address:lucio.frydman@weizmann.ac.il

[1] J.H. Ardenkjær-Larsen, B. Fridlund, A.Gram, G. Hansson, M.H. Lerche, R. Servin, M. Thaning, K. Golman, Proc. Nati. Acad. Sci. **10**, p.10158 (2003);
[2] J. Wolber et al., Nucl. Instrum. Methods Phys. Res., Sect. A, **526**, 173-181 (2004);
[3] K. Golman, R. in't Zandt, M. Thaning, Proc. Natl. Acad. Sci. USA, **103**, 11270-11275 (2006);
[4] C.G. Joo, K.N. Hu, J. Bryant, R. Griffin, J. Am. Chem. Soc., **128**, 9428-9432 (2006);
[5] S. Bowen and C. Hilty, Angew. Chem., Int. Ed., **47**, 5235-5237 (2008);
[6] J. Leggett et al., Phys. Chem. Chem. Phys., **12**, 5883-5892 (2010);
[7] J. Kurhanewicz et al., Neoplasia, **13**, 81 (2011);
[8] E.C. Reynhardt, G.L. High. J. Chem. Phys, **10**, Vol. 109, p. 4090 (1998); J. Chem. Phys., **10**, Vol. 109, 4100 (1998);
[9] A. Gruber, A. Dräbenstedt, C. Tietz, L. Fleury, J. Wrachtrup, C. von Borczyskowski, Science **276**, 2012 (1997);
[10] R.J. Epstein, F.M. Mendoza, Y.K. Kato, and D.D. Awschalom, Nature Physics **1**, 94 (2005);
[11] L. Childress, M.V. Gurudev Dutt, J.M. Taylor, A.S. Zibrov, F. Jelezko, J. Wrachtrup, P.R. Hemmer, and M.D. Lukin, Science **314**, 281 (2006);
[12] M.V. Gurudev Dutt et al., Science, Vol. 316, p. 1312 (2007);
[13] R. Hanson, V. Dobrovitski, A. Feigun, O. Gywat and D. Awschalom Science **320**, 352 (2008);
[14] J.M. Taylor, P. Cappellaro, L. Childress, L. Jiang, D. Budker, P.R. Hemmer, A. Yacoby, R. Walsworth, M.D. Lukin, Nature Phys. **4**, 810 (2008).
[15] J.R. Maze et al., Nature, **455**, 644 (2008);
[16] G. Balasubramanian et al., Nature, **455**, 648, (2008);
[17] V.M. Acosta, E. Bauch, A. Jarmola, L.J. Zipp, M.P. Ledbetter, D. Budker, Appl. Phys. Lett. **97**, 174104 (2010);
[18] V. Jacques, P. Neumann, J. Beck, M. Markham, D. Twitchen, J. Meijer, F. Kaiser, G. Balasubramanian, F. Jelezko, J. Wrachtrup, Phys. Rev. Lett., Vol. **102**, p. 057403 (2009);
[19] P. Neumann, J. Beck, M. Steiner, F. Rempp, H. Fedder, P.R. Hemmer, J. Wrachtrup, F. Jelezko, Science, Vol **329**, p. 542 (2010);
[20] J.P. King, P.J. Coles, J.A. Reimer, Phys. Rev. B, Vol. **81**, p. 073201, (2010);
[21] J.M. Cai, F. Jelezko, M.B. Plenio, A. Retzker, ArXiv, Vol 1112.5502 (2011);
[22] E. Togan, Y. Chu, A. Imamoglu, M.D. Lukin, Nature, Vol. **478**, p. 497 (2011);
[23] B. Smeltzer, L. Childress, A. Gali, New J. Phys. **13**, 025021 (2011);
[24] A. Dréau, J.-R. Maze, M. Lesik, J.F. Roch, and V. Jacques, Phys. Rev. B, **85**, 134107 (2012);
[25] B. Smeltzer, J. McIntyre, L. Childress, Phys. Rev. A, Vol. 80, 050302 (2009);
[26] L. Childress, Ph.D. Thesis, p. 52, Harvard University (2006);
[27] N.B. Manson, J.P. Harrison, M.J. Sellars, Phys. Rev. B, Vol. 74, p. 104303 (2006);
[28] M.W. Doherty, N.B. Manson, P. Delaney and L.C.L. Hollenberg, New Journal of Physics, Vol. 13, p. 025019 (2011);
[29] S. Felton, A.M. Edmonds, M.E. Newton, P.M. Martineau, D. Fisher, D.J. Twitchen, J.M. Baker, Phys. Rev. B, Vol 79, p. 075203 (2009);
[30] E.C. Reynhardt, C.J. Terblanche, Chem. Phys. Lett., **269**, 464-468, (1997);
[31] A. Dréau, P. Spinicelli, J.R. Maze, J.F. Roch, V. Jacquesar, arXiv:1210.6195v2 [quant-ph]

Supplementary Information: Bulk Nuclear Polarization Enhanced at Room-Temperature by Optical Pumping

Ran Fischer,[1] Christian O. Bretschneider,[2] Paz London,[1] Dmitry Budker,[3,4] David Gershoni,[1] and Lucio Frydman[2]

[1]*Department of Physics, Technion, Israel Institute of Technology, Haifa, 32000, Israel*
[2]*Department of Chemical Physics, Weizmann Institute of Science, Rehovot, 76100, Israel*
[3]*Department of Physics, University of California, Berkeley, CA, 94720-7300, USA*
[4]*Nuclear Science Division, Lawrence Berkeley National Laboratory, CA, 94720, USA*

I. THE POSITIONING AND ALIGNMENT PROCESS BY OPTICALLY DETECTED MAGNETIC RESONANCE (ODMR)

Fulfilling the excited-state level anti-crossing (ESLAC) conditions that enable the transfer between electronic and nuclear polarization requires - prior to proceeding with the optical pumping - positioning and accurately aligning the NV-doped diamond single crystal to one of the crystallographic axes of the diamond in a B_z ∼50 mT field. Due to the diamond's tetrahedral lattice structure, the angles between a given crystal axis (e.g. [1,1,1]) and the remaining three axes ([-1,1,1], [1,-1,1], [1,1,-1]) are identical. Hence, it can be assumed that, if an NV center axis is aligned parallel to the external magnetic field $\vec{B}$, the transition frequencies of the corresponding non-aligned NV centers' orientations will be identical. This effect can be exploited during the alignment process of the diamond single-crystal: if three individual ODMR resonance frequencies corresponding to different NV orientations are collapsed into a single line, the magnetic field will be aligned to a single orientation and the optical pumping efficiency will be maximized. The careful orientation

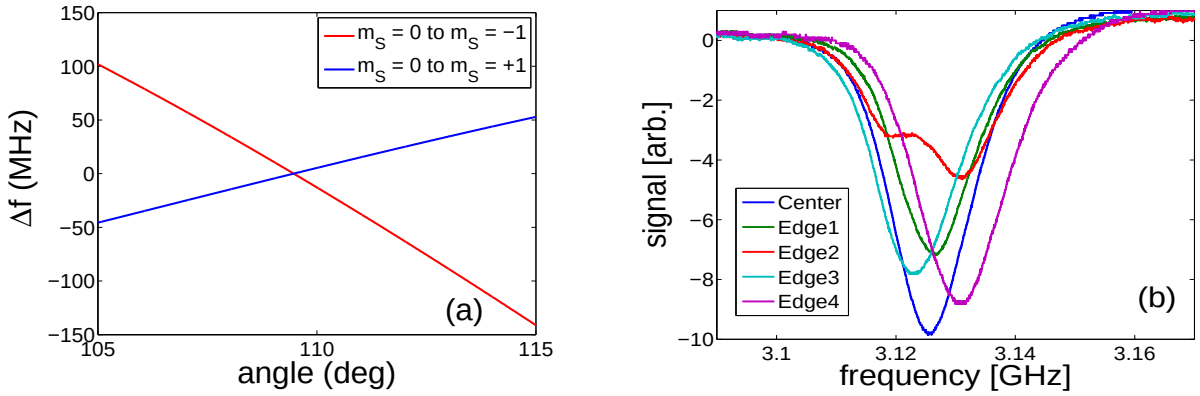

Supp. 1: (Color online) (a) Difference in transition frequencies within the ground-state at a magnetic field of 50 mT as a function of the angle between the NV center axis and the external magnetic field with an angle dependence of the transition m_s=0→1 (m_s=0→-1) of 10 (25) MHz/°. (b) ODMR measurements of the m_s=0→-1 transition of the three non-aligned orientations, at a field of ≈50 mT. The different curves correspond to the four edges and the center on the diamond sample.

of the crystal with respect to the magnetic field was guided by this premise, and it was physically modified by slight adjustments of a series of plastic setting screws within a custom-built goniometer attached to the sample holder. Figure Supp. 1(a) illustrates the sensitivities of the various ground-state transition frequencies at a magnetic field of ≈50 mT with respect to azimuthal orientation. With these principles guiding the alignment procedure, angular precisions better than 0.5° - corresponding to splittings of ∼20 MHz between the different NV orientations - are easily achieved. To estimate inhomogeneities in the magnetic field, we performed ODMR measurements targeting the four corners plus the center of the diamond sample. Judging from the residual splittings observed on the resonance lines (Supp. 1(b), illustrated by a corner position) it was concluded that an inhomogeneity of the magnetic field on the order of ∼0.1-0.2 mT in the axial and radial directions, characterized our fields throughout the diamond sample.

II. DENSITY MATRIX SIMULATION

Simulations of the kind illustrated in Fig. 1c, estimating the transfer of polarization between an electronic and a proximal nuclear spin ensemble as a function of the magnetic field, were based on calculating the temporal evolution of the spin

density matrix based on the Master equation

$$\frac{d}{dt}\hat{\rho} = \frac{1}{i\hbar}[\hat{H}, \hat{\rho}] + \mathfrak{L}\,\hat{\rho} = 0. \tag{1}$$

Hereby $\hat{\rho}$ was the density matrix of the joint manifold of the NV center triplet excited state ^{3}E, and a single proximal ^{13}C nuclear spin, $\hat{H}$ was the Hamiltonian of the system and $\mathfrak{L}$ was the Lindblad super-operator describing the relaxation mechanisms. The Hamiltonian used in the calculation is a given in the paper's Eq. (1) , while the relaxation super-operator can be written as

$$\mathfrak{L}\,\hat{\rho} = \sum_n \gamma_n^2 (\hat{C}_n\,\hat{\rho}\,\hat{C}_n^\dagger - \frac{1}{2}\hat{C}_n^\dagger\,\hat{C}_n\hat{\rho} - \frac{1}{2}\hat{\rho}\,\hat{C}_n^\dagger\,\hat{C}_n) \tag{2}$$

where γ_n are the decay rates associated with the relaxation processes, and C_n are the operators which determine the relaxation process - either decoherence or depopulation. The simulation started with setting conditions that enabled the establishment of a steady-state polarization, using only C_n operators. This can be carried out by considering that a given

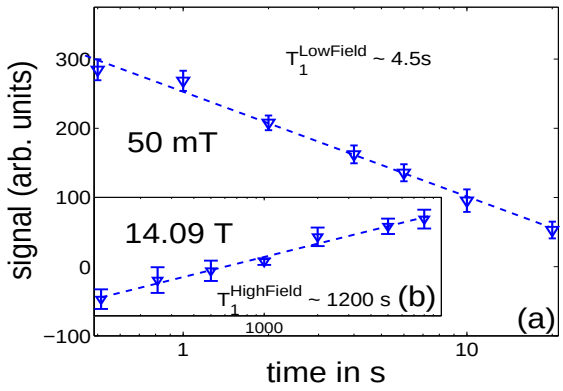

Supp. 2: (Color online) (a) Spin-lattice relaxation characteristics of optically pumped signal of the diamond sample D02 at a polarizing field of (B_z ∼50 mT, $T_1^{LowField}$ ∼4.5 s). (b) Relaxation time ($T_1^{HighField}$ ∼1200 s) obtained for a saturation-recovery experiment under thermal polarizing conditions in a high magnetic field (B_0 = 14.09 T). These spin-lattice relaxation times were measured in complete analogy with the methods and equipment used for the diamond crystal D01 (Fig. 3c, main manuscript)

$\hat{C}_n = \gamma_n\,|i\rangle\langle j|$ operator, will result in a net polarization transfer from state $|j\rangle$ to state $|i\rangle$. These "depopulation operators" can therefore account for the spin-lattice relaxation times T_1 of the electronic and/or nuclear systems, as well as for the optical pumping process. This was modeled by giving different decay rates γ_n for the operators $\hat{C}_0 = \gamma_0\,|0\rangle\langle\pm1|$ ($\hat{C}_{\pm1} = \gamma_{\pm1}\,|\pm1\rangle\langle0,\pm1|$) leading to population transfer from the m_s=±1→0 (m_s=0,±1→ ±1). The ratio of γ_0 and $\gamma_{\pm1}$ was set to '20' to create a steady-state population (∼0.9) consistent which experimental data [1]. The hyperfine interaction tensor utilized in these simulations was taken from [2]

$$A_{IS} = \begin{pmatrix} 5.0 & -6.3 & -2.9 \\ -6.3 & 4.2 & -2.3 \\ -2.9 & -2.3 & 8.2 \end{pmatrix} \tag{3}$$

in which all values are given in MHz. In order to mimic different orientations and magnitudes of the nuclear-electronic coupling throughout the diamond, we re-oriented the hyperfine tensor by a spatial rotation using Euler angles (α, β and γ). These rotation angles were chosen randomly to create the polarization plots displayed in Figure 1(c) of the main article.

ADDITIONAL EXPERIMENTAL DATA

The comparison of the obtained spin-lattice relaxation times for the samples D01 and D02 showed that both crystals exhibit comparable relaxation characteristics in low field (≈50 mT) environments, while at high fields these times differ by ca. an order of magnitude. The fluorescence data observed upon laser irradiation suggests that the concentration of NV

centers in D02 is ca. three times higher than in D01. These relaxation and fluorescence data indicate that paramagnetic effects caused by the presence of the NV centers does not play the dominant relaxation mechanism for bulk ensemble of ^{13}C spins.

[1] N.B. Manson, J.P. Harrison, M.J. Sellars, Phys. Rev. B **74**, 104303, (2006);
[2] L. Childress, Ph.D. Thesis, p. 52, Harvard University (2006);